JOURNAL OF GEOPHYSICAL RESEARCH, VOL. 101, NO. A5, PAGES 10,817–10,826, MAY 1, 1996

Detection of localized, plasma-depleted flux tubes or bubbles in the midtail plasma sheet

V. A. Sergeev,[1] V. Angelopoulos,[2,3] J. T. Gosling,[4] C. A. Cattell,[5] and C. T. Russell[6]

Abstract. Recent studies have shown that most Earthward transport in the midtail, high-beta plasma sheet takes place in the form of short-lived, high-speed plasma flow bursts. Bursty bulk flows are observed both when the plasma sheet is thin, such as during substorm expansion, and when it is thick, such as during substorm recovery. We present multi-instrument observations from the ISEE 1 and ISEE 2 spacecraft to argue that when the plasma sheet becomes thick and close to its equilibrium state, the plasma and magnetic field signatures of high-speed flow events are consistent with the theoretically predicted signatures of plasma-depleted flux tubes or "bubbles" [*Pontius and Wolf*, 1990; *Chen and Wolf*, 1993]. These signatures consist of a decrease in the plasma pressure and an increase in the B_z-component of the magnetic field accompanying the high speed flow. We show that the Earthward moving bubbles are separated from the plasma ahead of them by a sharp tangential discontinuity. The layer ahead of the bubbles exhibits flow and magnetic field shear consistent with flow around an Earthward moving obstacle. The bubble is in approximate total pressure balance with the surrounding medium. We show that there is a systematic difference in the orientation of the discontinuity measured at ISEE 1 and 2, implying a small (about 1-3 R_E) cross-tail size of the bubbles.

1. Introduction

In recent years it has become apparent that Earthward plasma convection in the tail plasma sheet takes place in an impulsive fashion; most Earthward transport of the plasma and magnetic flux occurs in the form of short-duration, high-speed plasma flows, rather than as a slow, steady convection [*Baumjohann et al.*, 1989; *Angelopoulos et al.*, 1994]. Such transient flow increases (hereby termed bursty bulk flows (BBFs), after *Angelopoulos et al.* [1992]) are a characteristic of plasma sheet convection not only during geomagnetically active times, but also during low-activity conditions. However, they are most frequent during high auroral electrojet (AE) activity [*Baumjohann*, 1993; *Angelopoulos et al.*, 1994] and persist even during steady magnetospheric convection events [*Sergeev et al.*, 1990].

The bursty bulk flows exhibit considerable variability of the order of 1 min or less. The origin of that variability is not understood. In particular, it is not clear whether the variability is due to local temporal variations of the ambient plasma or whether it is a manifestation of spatial propagation of individual plasma structures of varying plasma properties. However, it is noteworthy that the 1-min timescale of the individual high-speed flow bursts is typical for many other magnetotail and ionospheric phenomena [*Sergeev et al.*, 1992].

From the magnetotail processes discussed theoretically, at least two can be envisioned as possible representations of BBFs. One of them is impulsive magnetic reconnection [*Semenov et al.*, 1992]. *Sergeev et al.* [1987, 1992] showed that this model successfully describes certain features of the thinned plasma sheet observed during substorms around the time of flow reversal from tailward to Earthward. This mechanism may operate in thin current sheets with a small northward component of the ambient magnetic field B_z.

Under such conditions the magnetic stresses are responsible for the local acceleration of the plasma efficiently, in the absence of tail-aligned pressure gradients. Later, during the course of a substorm, B_z increases and Earthward plasma pressure gradients become essential. In such cases, other theoretical descriptions of the presence and evolution of flow bursts are necessary.

A second theoretical model that is a likely candidate for the description of fast flows in a dipolarized plasma sheet is one involving the plasma-depleted flux tubes or bubbles proposed by *Pontius and Wolf* [1990] and *Chen and Wolf* [1993]. This model predicts that an underpopulated plasma tube of small cross-tail size, after its formation, may intrude Earthward in the plasma sheet. This occurs due to the electric charging of the bubble which allows it to propagate through the plasma sheet without being quickly stopped by pressure gradients. Such structures have not yet been identified in the plasma sheet. When discussing the average signatures of the flow bursts found by *Angelopoulos et al.* [1992], *Chen and Wolf* [1993] found a principal disagreement with the bubble model, particularly that the plasma pressure did not show a clear decrease. They concluded that, if the bubbles exist, most of them probably stop outside the observation region (i.e. at $|X_{GSM}| > 20\ R_E$). Therefore the questions, (1) whether the bubbles really exist in the plasma sheet and (2) what is the theoretical description of bursty convection in the midtail plasma sheet (i.e., at $10 < |X| < 20$), remain unanswered.

The identification of plasma-depleted flux tubes in the midtail plasma sheet is the primary objective of this paper. It is based on multi-instrument observations by the ISEE 1 and 2 spacecraft. The paper is organized as follows: in section 2 we

[1]Institute of Physics, University of St. Petersburg, St. Petersburg, Russia.
[2]Applied Physics Laboratory, Johns Hopkins University, Laurel, Maryland.
[3]Now at Space Sciences Laboratory, University of California, Berkeley.
[4]Los Alamos National Laboratory, Los Alamos, New Mexico.
[5]School of Physics and Astronomy, University of Minnesota, Minneapolis.
[6]Institute of Geophysics and Planetary Physics, University of California, Los Angeles.

Paper number 96JA00460.
0148-0227/96/96JA-00460$09.00

show that BBFs are observed both when the current sheet is thin, as is typical at early substorm expansion, and when it is thick, as is typical during substorm recovery. In section 3, after a short discussion of the predictions of the bubble model, we describe several examples of isolated flow bursts in an expanded plasma sheet to show that they conform with the predictions of the bubble theory. We especially stress those aspects (generation of shear flows ahead of the bubble and cross-tail size of bubbles) which are important for the bubbles to intrude deep into the near-Earth plasma sheet. The results are discussed in section 4.

2. Observations: General Review

2.1. General Information

We used data from the University of Calfornia, Los Angeles (UCLA) fluxgate magnetometers on board the ISEE 1 and 2 satellites at 1 s resolution in GSM coordinates. We also used data from the Fast Plasma Experiment instrument (FPE) on board the ISEE 2 satellite, which measured the ion distribution function in the range 0.07-40 keV and provided information on the ion density, temperature, and flow velocity on the ecliptic plane in spacecraft (roughly GSE) coordinates at 12-s resolution (in low data rate transmission). We complemented these measurements with electric field measurements in the ecliptic plane from the double-probe experiment on board the ISEE 1 spacecraft. The convection velocity (**E**×**B**) can be computed from those measurements if $B_z > \sim 0.2\ (B_x^2+B_y^2)^{-1/2}$ in spacecraft coordinates [*Cattell and Mozer*, 1984]. During the events studied, ISEE 2 was always Earthward and dawnward from ISEE 1. The spacecraft separation varied between 0.5 and 1.3 R_E, while the Z_{GSM} separation was 0.3-0.4 R_E for all events, with ISEE 2 always southward of ISEE 1.

2.2. Overview of Plasma Sheet Observations During the Coordinated Data Analysis Workshop 6B Substorm Event

To put the observations into the context of substorm phenomenology, we show a series of bursty bulk flow events during a substorm on March 31, 1979. This substorm was studied during the sixth Coordinated Data Analysis Workshop (CDAW 6) [*McPherron and Manka*, 1985]. Electric field and convection data for this event have been discussed by *Pedersen et al.* [1985]. This example demonstrates many of the features which we attribute to bubbles. In GSM coordinates the spacecraft were at [-20., -4., 1.] R_E with a separation vector from ISEE 1 to ISEE 2 being $dS_{12} \sim$ [0.6, -0.2, -0.37] R_E. The bottom two panels of Figure 1 show the plasma bulk flow at ISEE 2 (V_{x2}) and the *Y* GSE component of the electric field at ISEE 1 (E_{y1}). Both parameters display a number of intense bursts between 1350 UT and 1610 UT. The ISEE spacecraft were northward of the neutral sheet at the beginning of event and crossed the neutral sheet many times between 1411 and 1533 UT.

The vertical separation of the two ISEE spacecraft makes it possible to monitor the current sheet density by comparing the values of B_x when at least one spacecraft was in the central part of the plasma sheet or when the spacecraft were on opposite sides of the current sheet [*Sergeev et al.*, 1992, 1993]. The difference $dB_x=B_{x1}-B_{x2}$ between the B_x component at the two spacecraft is plotted in the upper panel of Figure 1. It characterizes the amount of cross-tail current in a horizontal slab between two spacecraft.

The variations in dB_x indicate two quite different regions in the plasma sheet. For half an hour after substorm onset (i.e., from 1354 UT until 1430 UT) dB_x had values between 20 and 36 nT if times when both spacecraft were in the lobe and thus show little difference in B_x are excluded. This is comparable to the lobe field (about 22 nT at this time) and shows that nearly all of the plasma sheet current was pinched to a slab with half thickness of less than 0.3-0.4 R_E (i.e., less than the Z_{GSM} distance between ISEE 1 and 2). This corresponds to a current sheet density about 5-7 times larger than the average given by magnetospheric models; for example, in the *Tsyganenko* [1989] models, dB_x ranges between 4 and 9 nT for K_p between 2 and 5, for a spacecraft separation dZ=0.37 R_E. Later on during the substorm (i.e., after 1430 UT), dB_x was small, only a few nanoteslas, which is somewhat smaller than in these models. This corresponds to a thick plasma sheet formed in the midtail after substorm expansion and is typical of the plasma sheet behavior at the late expansion phase or recovery phase of substorms [*Pytte et al.*, 1978].

Intense, bursty variations of V_x and E_y are seen under both the thin and the thick plasma sheet conditions. Several short duration flow pulses are identified in the thin current sheet, including tailward flow of ~600 km/s magnitude (burst a) and an Earthward flow burst of similar magnitude (burst b) detected ~5 min later. The tailward flow burst a was accompanied by a distinct bipolar (north then south) magnetic variation in B_z at both spacecraft and a bipolar (dawn then dusk) E_y variation at ISEE 1. Near the lobe (ISEE 1) it was evidenced as an enhanced B_x field, similar to the well-known traveling compression regions (TCRs) [e.g., *Slavin et al.*, 1993]. In the plasma sheet (ISEE 2) it produced a pressure pulse in the leading part of the structure (during the northward B_z excursion) which is evident both in the ion as well as in the total pressure. The Earthward flow burst b was accompanied by the unipolar, northward B_z variation and duskward E_y electric field, although ISEE 2 in this episode was in the outer plasma sheet. The flow burst b was followed by another Earthward flow (burst c) during which ISEE 2 shortly approached the neutral sheet, still measuring an intense flow. Both bursts a and b had associated B_y variations, although the sign of the magnetic shear changed from negative to positive from burst a to burst b. These signatures are quite typical for the impulsive variations in the substorm-associated thin current sheet previously systematized by *Sergeev et al.* [1992].

Three episodes of high-speed (>600 km/s) flow bursts (f, g, and h) occurred in the expanding plasma sheet after 1430 UT. They were accompanied by an increased and fluctuating B_z and intense (up to 6 mV/m) bursts of positive E_y, both indicating enhanced magnetic flux transport. Each of these episodes actually consists of several 1-min timescale events, which is better seen in the variations of E_y and B_z presented at higher time resolution. As seen in the trace of the plasma pressure measured at ISEE 2 and presented in the central panel in Figure 1 ($P_{plasma2}$), these short-duration flux transfer events also have associated plasma pressure decreases; thus they constitute candidates for bubbles.

3. Analysis Of Bubble Events

3.1. Predictions of Bubble Model

Following the theoretical description given by *Pontius and Wolf* [1990] and *Chen and Wolf* [1993], who built upon the

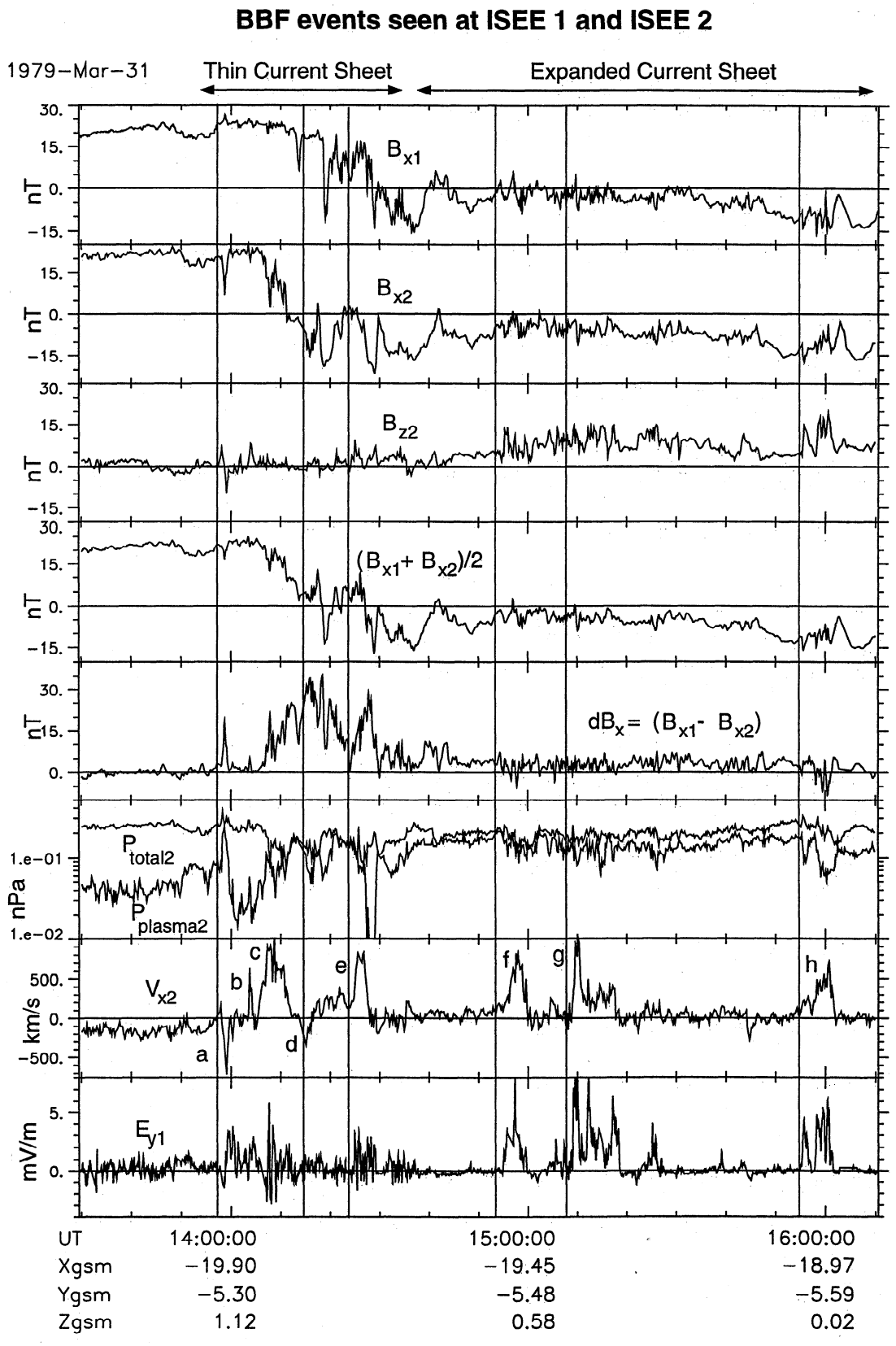

Figure 1. Summary plot of ISEE 1 and 2 observations on March 31, 1979.

earlier study of *Pontius and Hill* [1989], we briefly summarize the predictions of the bubble model to demonstrate which observational signatures are necessary to confirm the detection of a plasma bubble. Figure 2 is a schematic of the equatorial cross section of a bubble as viewed from north. The bubbles have been described as underpopulated flux tubes (having smaller value of PV^{γ}, where P is the plasma pressure and V is the flux tube volume) in pressure equilibrium with surrounding

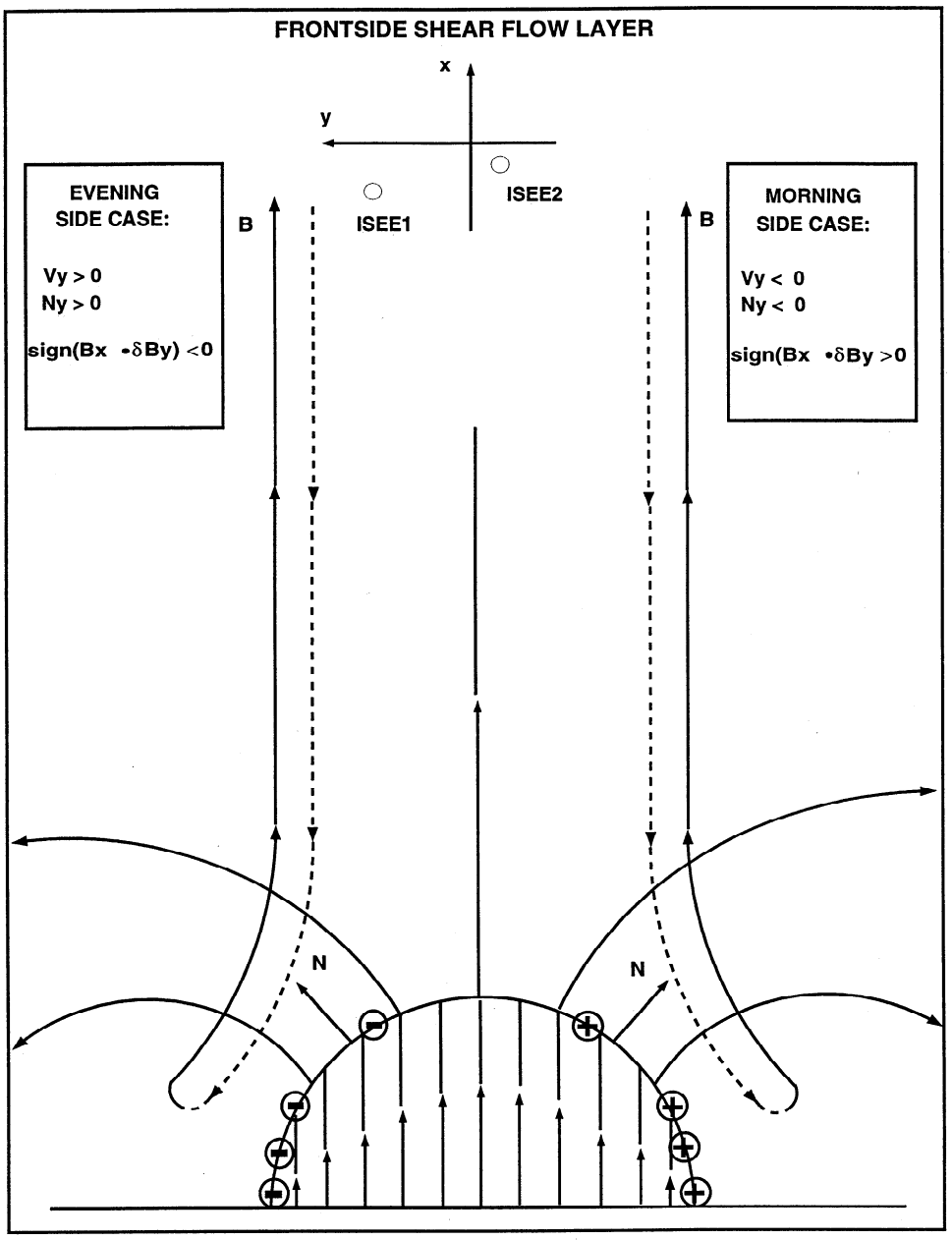

Figure 2. Schematic view (from the north) of the bubble proper and its frontside layer (adapted from *Pontius and Wolf* [1990, Figure 1]).

media. Owing to reduced plasma pressure and larger B, the cross-tail magnetic drift current inside the bubble is smaller than outside and the bubble is electrically polarized, as shown in Figure 2. Current continuity is accomplished either by an inertial current (while the electric charge is growing and the bubble is accelerating) or by field-aligned currents. The polarization electric field causes enhanced Earthward plasma flow inside the bubble proper and forces the background plasma to convect around the bubble. This scenario is depicted in a meridional view by *Chen and Wolf* [1993, Figures 3 and 4]. The equatorial cross section of the bubble and its surrounding flow is depicted in Figure 2, which is adapted from *Pontius and Wolf* [1990, Figure 1].

A shear flow pattern which develops ahead of the bubble is the principal mechanism which allows the deep Earthward intrusion of the bubble. This flow moves some of the plasma tubes ahead of the bubble around its flanks. The Y localization of this scenario is important because in a strictly two-dimensional configuration, there can be no flux tube interchange and thus no motion of plasma-depleted flux tubes Earthward. The flow pattern shown in Figure 2 allows the bubble to penetrate Earthward by displacing sideways the high, specific entropy plasma tubes ahead of it. The background magnetic flux tubes carried by the frontside shear flow are expected to be draped around the bubble, causing magnetic shear outside the equatorial plane, as shown in Figure 2.

The shear flow pattern is essentially a three-dimensional effect; it is possible only when the bubble cross-tail size is small. The inward motion of a large-scale (a sizable fraction of the tail cross section) bubble would cease quickly due to the pressure increase of the flux tubes ahead of it. On the other hand, *Chen and Wolf* [1993] postulated that the bubbles would

be larger than 1 R_E because bubbles of smaller size would be dissolved quickly due to the particle drifts. Finding the cross-tail size of the bubbles is an essential part of this paper. In summary, the main observational signatures by which plasma bubbles can be detected are as follows.

1. The plasma pressure P decreases and B_z increases within the bubbles. Fast Earthward flow is also expected inside the bubbles, but the flow magnitude depends on the bubble's evolutionary stage.

2. A flow shear layer will form ahead of and around the bubble. This flow shear layer may also contain magnetic shear. The sign of the magnetic shear should change on opposite sides of the neutral sheet and on opposite sides of the bubble (morningside versus eveningside), as shown in Figure 2.

3. The orientation of the bubble boundary may help confirm the bubble detection and characterize its cross-tail size. An estimate of the normal to the boundary can be obtained by using a principal axis analysis of the magnetic field [*Sonnerup and Cahill*, 1967]. In this method the normal to a plane-like discontinuity is defined as the direction in which the magnetic field variations are smallest. Knowledge of the front orientation helps define which side of the bubble (evening or morning) was encountered by the spacecraft. As seen in Figure 2, if the Y separation of two spacecraft is comparable to the cross-tail size of the bubble, one may expect large differences between the front orientations at the two spacecraft.

3.2. Two Examples of Isolated Bubbles

Several isolated bubbles were detected in the CDAW 6B substorm. Event h commencing at 1554 UT (Figure 3) consists of four bursts. Two of them (h1 and h2) have isolated onsets and will be described in detail. The leading structure (h1) displays a sharp increase of B_z in association with a drop in plasma pressure and density at ISEE 2. The latter features are confirmed by the increase in the absolute value of the spacecraft potential, V_{2S} recorded at ISEE 1, which corresponds to a decrease in the electron flux. The proton temperature also displayed a weak decrease. The frontside magnetic shear is evidenced by the short negative spikes in B_y centered at the beginning of the sharp increase in B_z. Its sign corresponds to the morningside crossing of the bubble boundary (negative dB_y with negative B_x, see Figure 2). This is also confirmed by the computed normals to the discontinuity h1 whose GSM azimuths are -18° and -32° at ISEE 1 and 2, respectively (see Table 1). The signatures in the plasma velocity are not large; the flow speed inside the bubble is moderate (~200 km/s). Weak signatures of negative V_y prior to the B_z discontinuity are also seen.

The second structure (h2) has very similar characteristics with the exception of larger effects in plasma flow; the flow speed inside the bubble exceeds the 400 km/s (threshold for identification of a bursty bulk flow event). A narrow, negative spike can be discerned in the 3-s resolution data of the Y component of the flow inferred from the electric and magnetic field on ISEE 1. This coincided with a similar, sharp negative spike in B_y.

In this event the magnetic variations are very similar at the spacecraft but they are delayed from ISEE 1 to ISEE 2, indicating an Earthward propagation of the magnetic structures. A cross-correlation analysis gave time delays of 8 and 5 s for the structures h1 and h2, implying propagation speeds along the average normal to each discontinuity of about 240 and 500 km/s, respectively.

During these events the absolute value of the X component of the magnetic field, $|B_x|$, increased during the B_z increase. One may attribute the simultaneous decrease in plasma pressure to an exit of the spacecraft from the plasma sheet (plasma sheet flapping), rather than to an encounter of a flux tube of different plasma pressure at the same distance from the neutral sheet. Tentative bubble encounters associated with a $|B_x|$ decrease (indicating motion toward the neutral sheet) could be attributed with less controversy to plasma bubble encounters. The next example of a plasma bubble has this property; i.e., a decrease in $|B_x|$ accompanying the B_z increase within the bubble.

The tentative bubble encounter took place at 1226 UT on April 17 during the late recovery phase of a substorm which commenced at about 1100 UT. Prior to 1226 UT the spacecraft were in the central plasma sheet (B_x about -10 nT, $N \sim 0.5$ cm^{-3} measuring weak Earthward flow ($V_x \sim 100$ km/s), as seen in Figure 4. At 1226 UT both spacecraft detected a sharp increase of B_z (from 4 to 13 nT in about 10 s), while both plasma pressure and density dropped by a factor of ~2.5. The spacecraft remained in the central plasma sheet, and the B_x field component decreased in absolute value. The total pressure (plasma plus magnetic pressure, including B_z component) displayed only a slight decrease. Despite the large magnetic field compression the temperature also decreased in this event. The Earthward flow reached a maximum speed of 500 km/s approximately one minute after the passage of the magnetic discontinuity and then decreased to a small value. The sharp B_z front was detected at ISEE 2 about 3-5 s later than at ISEE 1, confirming the Earthward propagation of this structure.

An obvious feature of this event is a 2-min-long episode of enhanced magnetic shear (spike of positive B_y) starting 1 min prior to the passage of the B_z discontinuity. It was accompanied by a similar (in phase and shape) spike of positive V_y component of plasma flow. The maximum speed in V_y (~400 km/s) was recorded during the passage of the B_z front. This is a good example of the frontside shear layer. According to predictions of section 3.1 and Figure 2, the positive V_y as well as the positive dB_y (for negative B_x) both correspond to the case of crossing the eveningside boundary of a localized bubble. The normals to the discontinuity derived from the principal axis analysis confirm this hypothesis, showing also that the front normal had a large angle (~60°) with the tail axis (see Table 1).

The major difference between the two events considered in this section lies in the behavior of the B_x component. In the April 17, 1979, event the spacecraft were closer to the current sheet center than in event h of March 31, 1979. In retrospect we note that during the March 31, 1979, events, $|B_x|$ increased together with B_z at the time of the discontinuity, but the relative increase was larger in B_z than in $|B_x|$. The magnetic field became more dipolar after the discontinuity in that event as well as in the April 17, 1979, event. Therefore, in both cases, one can discern a dipolarization of the magnetic field inside the bubble structure compared to the background.

3.3. Analysis of Discontinuities and Some Statistics

Using 1-s resolution magnetometer data, we defined the principal axis of covariance matrix for the frontside magnetic discontinuities for a number of isolated bubble events having sharp leading fronts. We used the updated version of the minimum variance analysis technique [*Sonnerup and Cahill*, 1967], as described by *Kawano and Higuchi* [1995]. The time intervals analyzed included the B_z discontinuity (from the

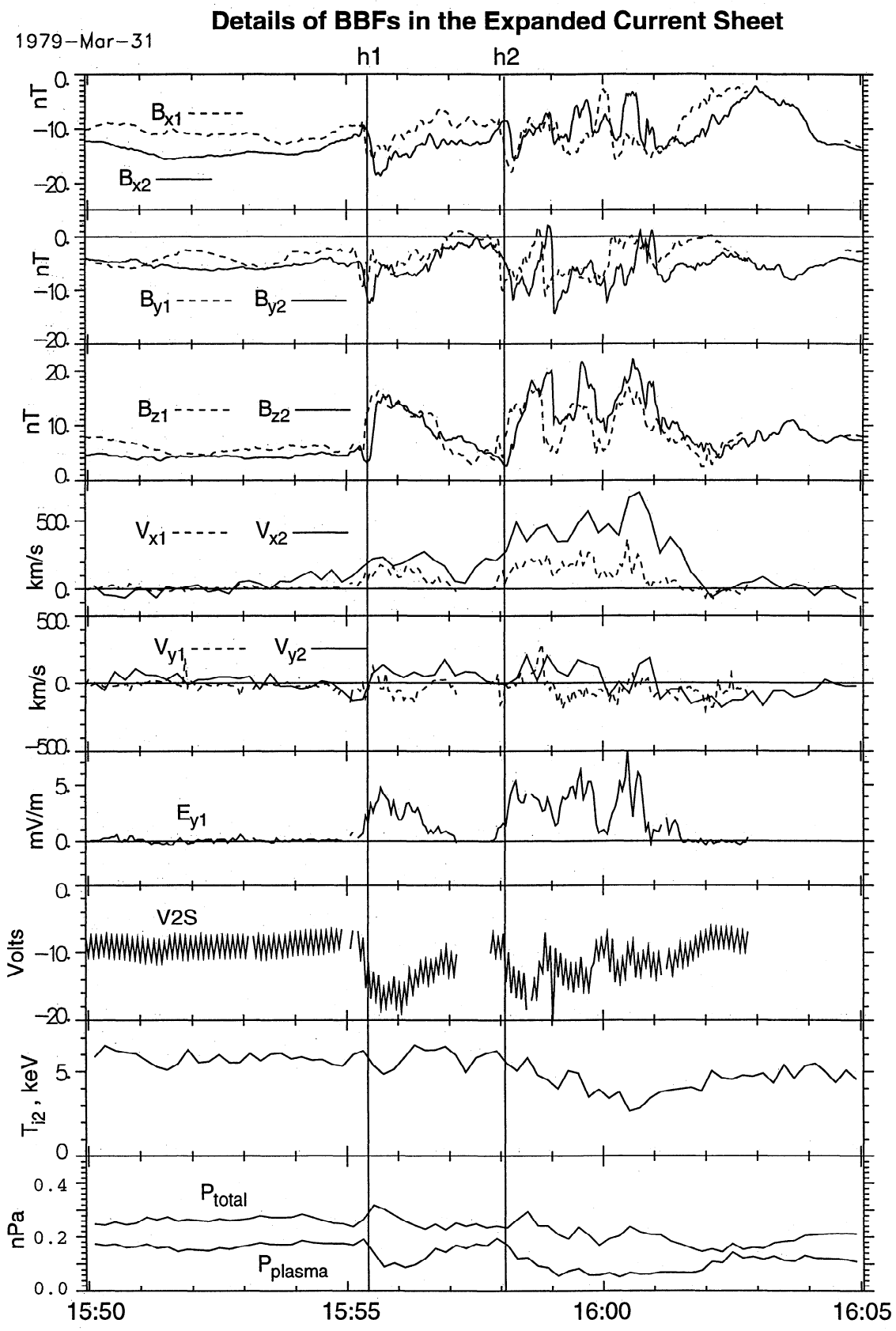

Figure 3. Detailed view of event h on March 31, 1979.

Table 1. Results of Minimum Variance Analysis of Bubble Frontside Discontinuities

Event	ISEE	N_3	L_2/L_3	B_3, nT	α	($\Delta\alpha$), deg	α_1-α_2, deg	Δt_{cc}, s	Δt_d, s	V_n, km/s	$D=\Delta t_d \times V_n$, R_E
Mar 31, 1979	1	[0.87, 0.31, 0.38]	23.0	1.4 (0.7)	20	(7)	22	15	13	127	0.26
Event f	2	[0.91, -0.03, 0.41]	20.0	-1.9 (0.7)	-2	(7)			14	166	0.36
Mar 31, 1979	1	[0.67, 0.67, 0.36]	17.0	0.9 (1.0)	46	(7)	13	8	37	83	0.48
Event g	2	[0.64, 0.41, 0.65]	13.0	1.9 (0.8)	33	(10)			21	33	0.11
Mar 31, 1979	1	[0.76, -0.24, 0.61]	4.1	-1.4 (4.3)	-18	(21)	14	8	10	260	0.41
Event h1	2	[0.65, -0.40, 0.65]	14.0	-0.2 (2.7)	-32	(12)			10	214	0.33
Mar 31, 1979	1	[0.53, -0.58, 0.61]	2.7	2.1 (5.8)	-48	(29) ?	16	5	8	? 303	0.38
Event h2	2	[0.43, -0.88, -0.21]	1.8	-0.5 (11.0)	-64	(31) ?			? 23	? 698	?
Apr 17, 1979	1	[0.46, 0.88, -0.12]	4.2	-0.6 (1.0)	62	(15) ?	1	4	9	?	?
	2	[0.48, 0.88, 0.03]	12.0	1.7 (1.4)	61	(8) ?			14	?	?

N_3 is the direction of normal to the discontinuity in GSM coordinates. L_2/L_3 is the ratio of intermediate to minimum eigenvalues. B_3 is the average magnetic field along the normal direction (values in parentheses are nanoteslas). Angle α is the azimuth of N_3 in GSM coordinates. Δt_{cc} is the intersatellite time delay in the magnetic signal estimated from a cross-correlation analysis; Δt_d is the duration of the sharp B_z increase. V_n is the velocity of the discontinuity along the normal. Numbers in parentheses are the standard deviation estimate. Question marks indicate large uncertainty.

minimum B_z value to its first maximum) with the addition of 5-s intervals on both sides. The results are given in Table 1. Positive time lag means propagation from ISEE 1 to ISEE 2, i.e., Earthward transport of the magnetic structure. The ratio of the intermediate to the minimum eigenvalues L_2/L_3 is also given in Table 1. The large values of that ratio indicate that the normals to the discontinuities are well defined. Results of the cross correlation between ISEE 1 and ISEE 2 are also included in Table 1 as well as some other characteristics of bubbles.

The discontinuities studied are sharp; their duration is typically of order of 10 s. With estimated propagation speeds of ~200 km/s, this implies a thickness about 0.3 R_E (see Table 1), which is an order of magnitude smaller than the average plasma sheet thickness. This justifies the local analysis of the structures as nearly planar discontinuities. In this case the direction of the minimum variance (unit vector N_3) defines the normal to the magnetic field discontinuity.

The average magnetic field along this direction (B_3, along the normal) is important in order to characterize the type of discontinuity and the processes of its formation. In practically all cases studied, this B_3 value is very small, nearly zero (taking into account the estimated errors given in parenthesis in Table 1). This leaves two options for identification, fast shock or tangential discontinuity. However, the structure cannot be a fast shock since both the plasma velocity behind the discontinuity and its apparent speed (V_d in Table 1) are about 100-400 km/s, i.e., much smaller than the sound speed in the plasma sheet (>1000 km/s). The interpretation of the frontside discontinuity as a tangential discontinuity is the only alternative, and that is compatible with the bubble model (contact surface of two flux tubes carrying different plasma populations).

The angles α_1 and α_2 in Table 1 characterize the projection of the normal (N_3) to the GSM XY plane as obtained for ISEE 1 and ISEE 2. These angles deviate considerably from 0 (up to 60° or so, much larger than the possible errors), showing that the discontinuities are not tangent to the tail axis. If we interpret these crossings as encounters with the flanks of localized structures, the sign of this angle indicates which edge (the morningside or the eveningside) was crossed by the spacecraft. Comparison of three different methods to specify the edge (morning or evening), based on the bubble model, shows a good agreement between them (Table 2).

The normals to the bubble front computed at the two spacecraft allow us to check how localized the bubbles are in the dawn-dusk direction. As seen from Table 1, there is a very systematic difference α_1-α_2 about 10°-20° between the normals at two spacecraft. Its positive sign is just what is expected, considering that ISEE 1 is duskward of ISEE 2 and should have a larger angle counted from the positive X axis (see Figure 2 for illustration). This implies a small cross-tail size of the bubble, comparable but greater than the Y separation of 0.2-0.4 R_E between the two spacecraft. For a circular shape of the frontside boundary, a spacecraft separation of 0.3 R_E and an angular difference 15° between normals, the diameter of the structure is 2.2 R_E. This indicates that the cross-tail size of the bubbles is about 1-3 R_E.

4. Discussion And Conclusions

We presented observations that confirm the theoretical hypothesis that in the midtail plasma sheet one may observe short-term flux transfer events which have the basic properties of bubbles, as described by *Pontius and Wolf* [1990], *Chen and Wolf* [1993], and in Section 3.1. Three main theoretical predictions, (1) plasma pressure decrease and B_z increase in the bubble core, (2) frontside flow shear layer, and (3) small cross-tail size of the bubbles, have been confirmed using data from two ISEE spacecraft at high temporal resolution.

There are several pieces of evidence in favor of the cross-tail localization of the bubble-like structures. First, the normals to the discontinuity ahead of the bubbles may deviate considerably from the Sun-Earth line, indicating an encounter with the edge of a localized structure. Second, the characteristics of individual short-term structures may correspond to the encounter with either morningside or eveningside edges, even if these structures are observed during the same event, i.e., at roughly the same satellite position. For example, during the CDAW 6B substorm, the characteristics of events f and g correspond to the crossings of the edge in the evening side (Tables 1 and 2), whereas events h1 and h2 correspond to crossings of the edge in the

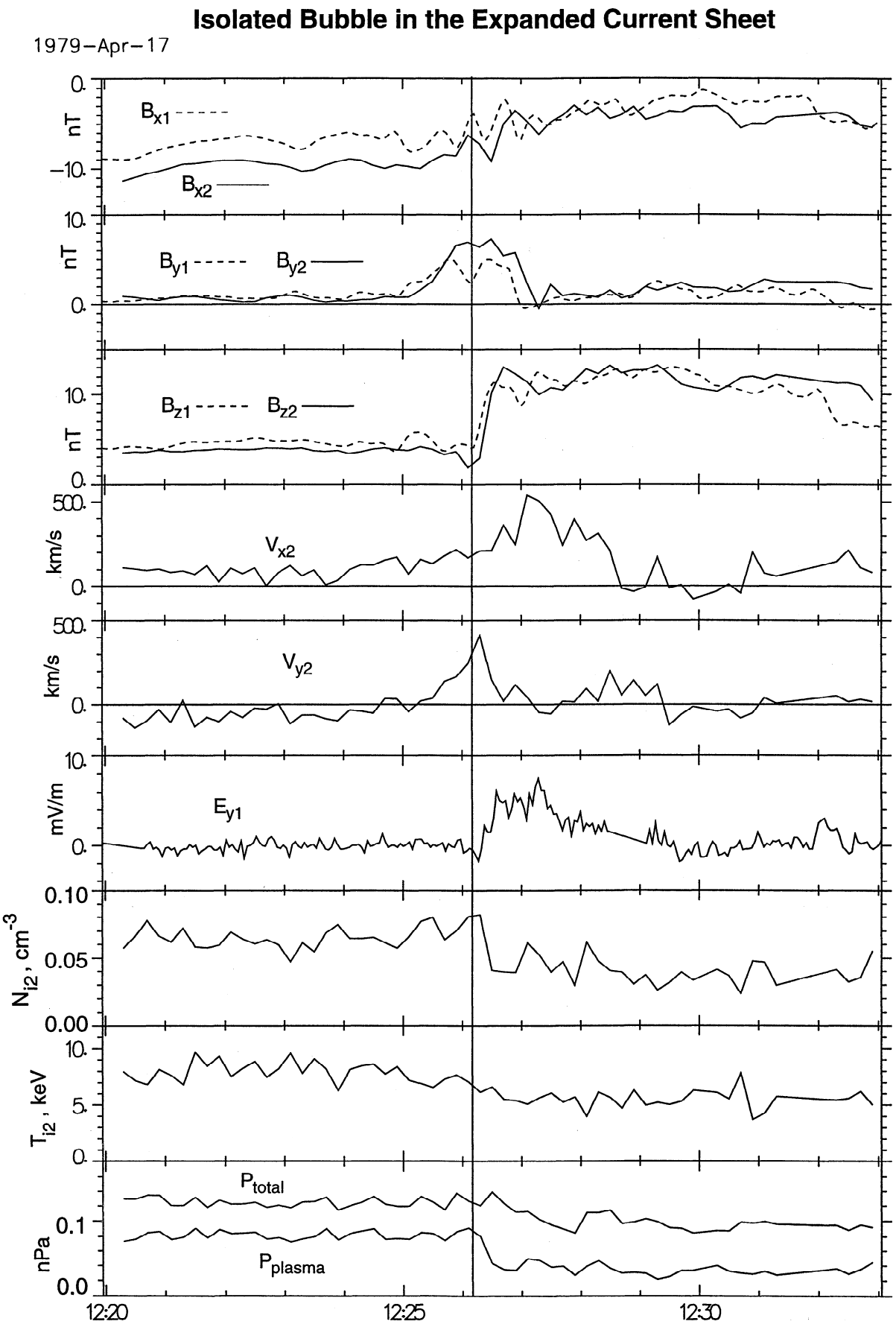

Figure 4. Detailed view of another isolated bubble on April 17, 1979.

Table 2. Identification of Bubble Edge (Morningside or Eveningside) by Three Different Methods

Event	N_{y3}†	$dB_y \times B_x$‡	dV_y*
March 31, 1979, f	E?	E	?
March 31, 1979, g	E	E	?
March 31, 1979, h1	M	M	M
March 31, 1979, h2	M	M	M
April 17, 1979	E	E	E

N_{y3} represents the Y_{GSM} component of the directional discontinuity normal computed from minimum variance analysis on the magnetic field. $dB_y \times B_x$ represents the B_y perturbation in the flow shear layer times the X_{GSM} component of the magnetic field. dV_y represents the V_y perturbation in the flow shear layer.

†First method is eveningside (E) (or morningside (M)) edge if $N_{y3}>0$ (<0).
‡Second method is eveningside (or morningside) edge if $dB_y \times B_x<0$ (>0).
*Third method is eveningside (or morningside) edge if $dV_y>0$ (<0).

morningside. Third, and most important, there is a systematic difference between the orientations of the normal to the discontinuity at two closely spaced ISEE spacecraft. This difference allowed us to estimate the bubble size as 1-3 R_E.

A preliminary survey showed that bubble-like structures are quite common in the expanded plasma sheet during the recovery phase of substorms but can also be encountered during non-substorm times (including quiet times and steady convection periods). Possible examples of plasma-depleted flux tubes during a steady convection event have been shown by *Sergeev et al.* [1990], based on ISEE observations. These authors focused on the short-term, high-speed flows associated with sharp B_z increases in the midtail plasma sheet at 20 R_E during a steady convection period. Two events with sharp B_z fronts analyzed in detail exhibited an Earthward propagation of magnetic structures (V_d ~ 400 km/s) as well as a weak magnetic field component along the discontinuity normal (B_3 ~ 2 nT). Although the plasma parameters from the FPE instrument were not available, the authors reported associated changes of the spacecraft potential V_{2S} indicating a decrease of the electron flux in the core of the high-speed structure. These properties are the same as we found in our study.

The ionospheric signatures of the events studied by *Sergeev et al.* [1990] were later investigated using a two-dimensional magnetometer network and the STARE radar to show that the associated enhancements of equatorward convection in the ionosphere have a limited local time extent of about 1 hour in magnetic local time (MLT) (see, e.g., the review by *Sergeev et al.* [1995, Figure 15]). Taking into account that 1 hour of MLT, mapped to the midtail according to the *Tsyganenko* [1989] model, corresponds to about 4 R_E width across the tail, this ionospheric observation is compatible with our estimate of the cross-tail size of the bubble.

Moortgat et al. [1990] analyzed a number of sharp magnetic field compression events observed by the ISEE spacecraft at 8-13 R_E distance with the purpose of checking whether they may be the manifestation of the Earthward propagating fast shocks. The results were negative concerning the shock identification: the compression structures had associated plasma flow speeds much less than the sound speed and, in the majority of the events, the authors found a decrease (rather than an increase) of the density after the discontinuity. These properties, however, are just the same as the characteristics of bubble structures found in our study. This implies that some bubbles may penetrate even into the near-tail region. Our preliminary survey has confirmed that bubble-like structures can be encountered as close to Earth as $|X|<10\ R_E$.

Our results indicate that some bubbles have a high enough plasma speed in the bubble core (>400 km/s) to be classified as bursty bulk flow events. However, slow-speed bubbles may also contribute significantly to magnetic flux transport (compare, for example, events h1 and h2 in the E_y trace of Figure 3). Therefore not every bubble belongs to the bursty bulk flow category, as some of them have only a moderate flow speed (100/200 km/s). There may be several factors which control the flow speed inside the bubble. One of them is the contrast between the specific entropy (PV^γ) in the bubble and the surrounding media which, according to the bubble theory, defines the imbalance of the corresponding magnetic drift currents. This imbalance leads to the polarization of the bubble. The intensity of the polarization electric field depends also on the processes controlling the intensity of the field-aligned currents which discharge the bubble. We observed that events having a similar contrast in B_z and plasma pressure (e.g., events h1 and h2) may have as much as a factor of 2 difference in velocity within the bubble core.

In addition to plasma bubbles, BBFs probably include other structures that have different characteristics. An example is the tailward flowing plasmoid-like structure at 1358 UT during CDAW 6B substorm (Figure 1) and other similar structures [*Lin et al.*, 1991; *Sergeev et al.*, 1987, 1992, 1995; *Angelopoulos et al.*, 1996]. Such structures were interpreted as evidence of impulsive magnetic reconnection or impulsive magnetotail acceleration. As the signatures of different phenomena are mixed in the superimposed epoch analysis of all fast flow bursts [*Angelopoulos et al.*, 1992], this may explain why the average pressure and density traces differs from those corresponding to individual bubble events.

To conclude, we presented observations of a few short-lived flux transfer events which have the basic signatures of plasma depleted flux tubes (bubbles). We also found that the bubbles have a cross-tail size of about 1-3 R_E and may be important constituents of Earthward flux transport in the magnetotail. Future studies have to address quantitatively the role of the bubbles in the Earthward transport and provide more detailed information on the physical properties of individual bubbles. This may be a challenging issue for forthcoming multispacecraft missions like Cluster and Interball.

Acknowledgments. V. A. was supported by NASA grant NAGW-4020. V. A. S. was financially supported by the INTAS grant N93-2031 as well as by the Russian Fund for support of Basic Research and by NASA grant NAGW-4020 during his visit to the Applied Physics Laboratory. Work at Los Alamos was performed under the auspices of the U.S. Department of Energy with support from NASA.

The Editor thanks B.U.O. Sonnerup and another referee for their assistance in evaluating this paper.

References

Angelopoulos, V., W. Baumjohann, C. F. Kennel, F. V. Coroniti, M. G. Kivelson, R. Pellat, R. J. Walker, H. Luhr, and G. Paschmann, Bursty

bulk flows in the inner central plasma sheet, *J. Geophys. Res., 97*, 4027, 1992.

Angelopoulos, V., C. F. Kennel, F. V. Coroniti, R. Pellat, M. G. Kivelson, R. J. Walker, C. T. Russell, W. Baumjohann, W. C. Feldman, and J. T. Gosling, Statistical characteristics of bursty bulk flow events, *J. Geophys. Res., 99*, 21,257, 1994.

Angelopoulos, V., *et al.*, Multipoint analysis of a bursty bulk flow event on April 11, 1985, *J. Geophys. Res., 101*, 4967, 1996.

Baumjohann, W., The near-Earth plasma sheet: An AMPTE/IRM perspective, *Space Sci. Rev., 64*, 141, 1993.

Baumjohann, W., G. G. Paschmann, and C. A. Cattell, Average plasma properties in the central plasma sheet, *J. Geophys. Res., 94*, 6597, 1989.

Cattell, C. A., and F. S. Mozer, Substorm electric fields in the magnetotail, in *Magnetic Reconnection in Space and Laboratory plasmas, Geophys. Monog. Ser., vol. 30*, edited by E.W. Hones Jr., p. 208, American Geophysical Union, Washington, DC , 1984.

Chen, C. X., and R. A. Wolf, Interpretation of high-speed flows in the plasma sheet, *J. Geophys. Res., 98*, 21,409, 1993.

Kawano, H., and T. Higuchi, The bootstrap method in space physics: Error estimation for the minimum variance analysis, *Geophys. Res. Lett., 22*, 307, 1995.

Lin, N., R. L. McPherron, M. G. Kivelson, and R. J. Walker, Multipoint reconnection in the near-Earth magnetotail: CDAW 6 observations of energetic particles and magnetic field, *J. Geophys. Res., 96*, 19,427, 1991.

McPherron, R. L., and R. H. Manka, Dynamics of the 1054 UT March 22, 1979, substorm event: CDAW 6, *J. Geophys. Res., 90*, 1175, 1985.

Moortgat, K. T., C. A. Cattell, F. S. Mozer, and R. Elphic, On the search for evidence of fast mode compressions in the near-Earth tail: ISEE observations, *J. Geophys. Res., 95*, 18,887, 1990.

Pedersen, A., C. A. Cattell, C.-G. Falthammar, K. Knott, P.-A. Lindqvist, R. H. Manka, and F. S. Mozer, Electric fields in the plasma sheet and plasma sheet boundary layer, *J. Geophys. Res., 90*, 1231, 1985.

Pontius, D. H., Jr., and T. W. Hill, Rotation driven plasma transport: The coupling of macroscopic motion and microdiffusion, *J. Geophys. Res., 94*, 15,041, 1989.

Pontius, D. H., Jr., and R. A. Wolf, Transient flux tubes in the terrestrial magnetosphere, *Geophys. Res. Lett., 17*, 49, 1990.

Pytte, T., R. L. McPherron, E. W. Hones Jr., and H. I. West Jr., Multiple-satellite studies of magnetospheric substorms: Distinction between polar magnetic substorms and convection-driven negative bays, *J. Geophys. Res., 83*, 663, 1978.

Semenov, V. S., I. V. Kubyshkin, V. Lebedeva, M. V. Sidneva, H. K. Biernat, M. F. Heyn, B. P. Besser, and R. P. Rijnbeek, Time-dependent localized reconnection of skewed magnetic fields, *J. Geophys. Res., 97*, 4251, 1992.

Sergeev, V. A., V. S. Semenov, and M. V. Sydneva, Impulsive reconnection in the magnetotail during substorm expansion, *Planet. Space Sci., 35*, 1199, 1987.

Sergeev, V. A., O. A. Aulamo, R. L. Pellinen, M. K. Vallinkoski, T. Bosinger, C. A. Cattell, R. C. Elphic, and D. J. Williams, Non-substorm short-lived injection events in the ionosphere and magnetosphere, *Planet. Space Sci., 38*, 231, 1990.

Sergeev, V. A., R. C. Elphic, F. S. Mozer, A. Saint-Marc, and J. Sauvaud, A two-satellite study of nightside flux transfer events in the plasma sheet, *Planet. Space Sci., 40*, 1551, 1992.

Sergeev, V. A., D. G. Mitchell, C. T. Russell, and D. J. Williams, Structure of the tail plasma/current sheet at 11 Re and its changes in the course of a substorm, *J. Geophys. Res., 98*, 17,345, 1993.

Sergeev, V. A., V. Angelopoulos, D. G. Mitchell, and C. T. Russell, In situ observations of magnetotail reconnection prior to the onset of a small substorm, *J. Geophys. Res., 100*, 19,121, 1995.

Slavin, J. A., M. F. Smith, E. L. Mazur, D. N. Baker, E. W. Hones Jr., T. Iyemori, and E. W. Greenstadt, ISEE 3 observations of traveling compression regions in the Earth's magnetotail, *J. Geophys. Res., 98*, 15,425, 1993.

Sonnerup, B. U. O., and L. J. Cahill Jr., Magnetopause structure and attitude from Explorer 12 observations, *J. Geophys. Res., 72*, 171, 1967.

Tsyganenko, N. A., A magnetospheric magnetic field model with a warped tail current sheet, *Planet. Space Sci., 37*, 5, 1989.

V. Angelopoulos, Space Sciences Laboratory, University of California, Berkeley, CA 94720-7450. (email: vassilis@ssl.berkeley.edu)

C. A. Cattell, Tate Laboratory of Physics, School of Physics and Astronomy, University of Minnesota, Minneapolis , MN 55455.

J. T. Gosling, D466, Los Alamos National Laboratory, P.O. Box 1663, Los Alamos, NM 87545.

C. T. Russell, Institute of Geophysics and Planetary Physics, 405 Hilgard Avenue, University of California, Los Angeles , CA 90095-1567.

V. A. Sergeev, Institute of Physics, University of St. Petersburg, Stary Petergof, St. Petersburg, 198904 Russia. (email: sergeev@space.phys.lgu.spb.su)

(Received September 28, 1995; revised February 6, 1996;
accepted February 6, 1996.)